

# Tumor Microenvironment and Its Clinicopathologic and Prognostic Association in Cutaneous and Noncutaneous Angiosarcomas

Isidro Machado, MD, PhD,<sup>1,2</sup> Celia Requena, MD,<sup>3</sup>  
Raquel López-Reig, PhD,<sup>4</sup> Antonio Fernández-Serra, PhD,<sup>4</sup>  
Francisco Giner, MD, PhD,<sup>5</sup> Julia Cruz, MD, PhD,<sup>1</sup> Victor Traves, MD,<sup>1</sup>  
Javier Lavernia, MD,<sup>6</sup> Reyes Claramunt, PhD,<sup>4</sup> Beatriz Llombart, MD, PhD,<sup>3</sup>  
José Antonio López-Guerrero, PhD,<sup>4</sup> and Antonio Llombart-Bosch, MD, PhD<sup>7</sup>

From the <sup>1</sup>Pathology Department, <sup>2</sup>Dermatology Department, <sup>3</sup>Laboratory of Molecular Biology, and <sup>6</sup>Oncology Unit, Instituto Valenciano de Oncología, Valencia, Spain; <sup>4</sup>Patologika Laboratory, Hospital QuirónSalud, Valencia, Spain; <sup>5</sup>Pathology Department, University Hospital, La Fe, Valencia, Spain; and <sup>7</sup>Pathology Department, University of Valencia, Valencia, Spain.

## ABSTRACT

**Objectives:** We explored features of the angiosarcoma (AS) tumor microenvironment to discover subtypes that may respond to immunotherapy.

**Methods:** Thirty-two ASs were included. Tumors were studied by histology, immunohistochemistry (IHC), and gene expression profile using the HTG EdgeSeq Precision Immuno-Oncology Assay.

**Results:** Comparing cutaneous and noncutaneous ASs, the second group showed 155 deregulated genes, and unsupervised hierarchical clustering (UHC) delineated two groups: the first mostly cutaneous AS and the second mainly noncutaneous AS. Cutaneous ASs showed a significantly higher proportion of T cells, natural killer cells, and naive B cells. ASs without *MYC* amplification revealed a higher immunoscore in comparison with ASs with *MYC* amplification. PD-L1 was significantly overexpressed in ASs without *MYC* amplification. UHC showed 135 deregulated genes differentially expressed when comparing ASs from the non-head and neck area with patients who had AS in the head and neck area. ASs from the head and neck area showed high immunoscore. *PD1/PD-L1* content was significantly more highly expressed in ASs from the head and neck area. IHC and HTG gene expression profiling revealed a significant correlation between PD1, CD8, and CD20 protein expression but not PD-L1.

**Conclusions:** Our HTG analyses confirmed a high degree of tumor and microenvironment heterogeneity. Cutaneous ASs, ASs without *MYC* amplification, and ASs located in the head and neck area seem to be the most immunogenic subtypes in our series.

## INTRODUCTION

Angiosarcomas (ASs) represent a heterogeneous group of vascular sarcomas that can arise in different organs with a variety of features. They occur more frequently in skin and soft tissue but appear also in the breast, bone, and viscera.<sup>1-7</sup> Commonly, ASs are aggressive tumors with frequent local recurrence and the potential for lymph node and distant metastases.<sup>7-16</sup> Primary and secondary ASs have been reported.<sup>1-5</sup> The first represent the majority of cutaneous

## KEY POINTS

- There is a high degree of tumor and microenvironment heterogeneity in cutaneous and noncutaneous angiosarcomas.
- Cutaneous angiosarcomas, angiosarcomas without *MYC* amplification, and angiosarcomas located in the head and neck area seem to be the most immunogenic subtypes.
- The implementation of an immunohistochemistry-based screening tool as a surrogate for immunologic gene profiling could be helpful to identify angiosarcomas susceptible to immunotherapy.

## KEY WORDS

Angiosarcoma; Molecular biology; RNA-seq; Immunoscore

*Am J Clin Pathol* XXXX 2023;XX:1-0  
[HTTPS://DOI.ORG/10.1093/AJCP/AQAD003](https://doi.org/10.1093/ajcp/aqad003)

Received: October 30, 2022  
Accepted: January 9, 2023

Corresponding author: Isidro Machado, MD, PhD; [isidro.machado@uv.es](mailto:isidro.machado@uv.es).



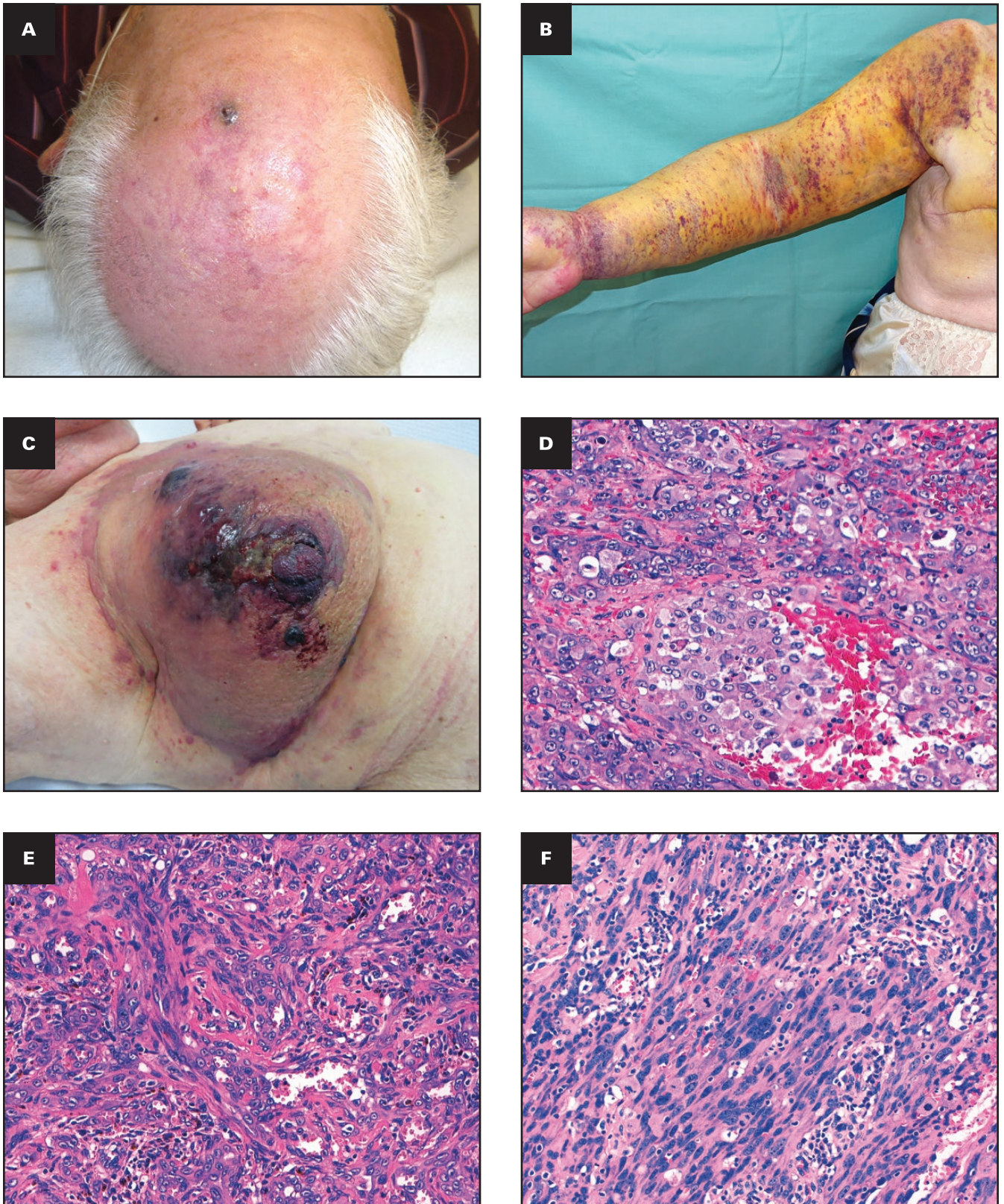


**FIGURE 1** **A**, Head and neck angiosarcoma. **B**, Lymphedema-associated angiosarcoma. **C**, Postradiation therapy angiosarcoma. **D**, Epithelioid cutaneous angiosarcoma (H&E,  $\times 20$ ). **E**, Angiosarcoma with spindle cells (H&E,  $\times 20$ ). **F**, Mitoses in high-grade angiosarcoma (H&E,  $\times 40$ ).

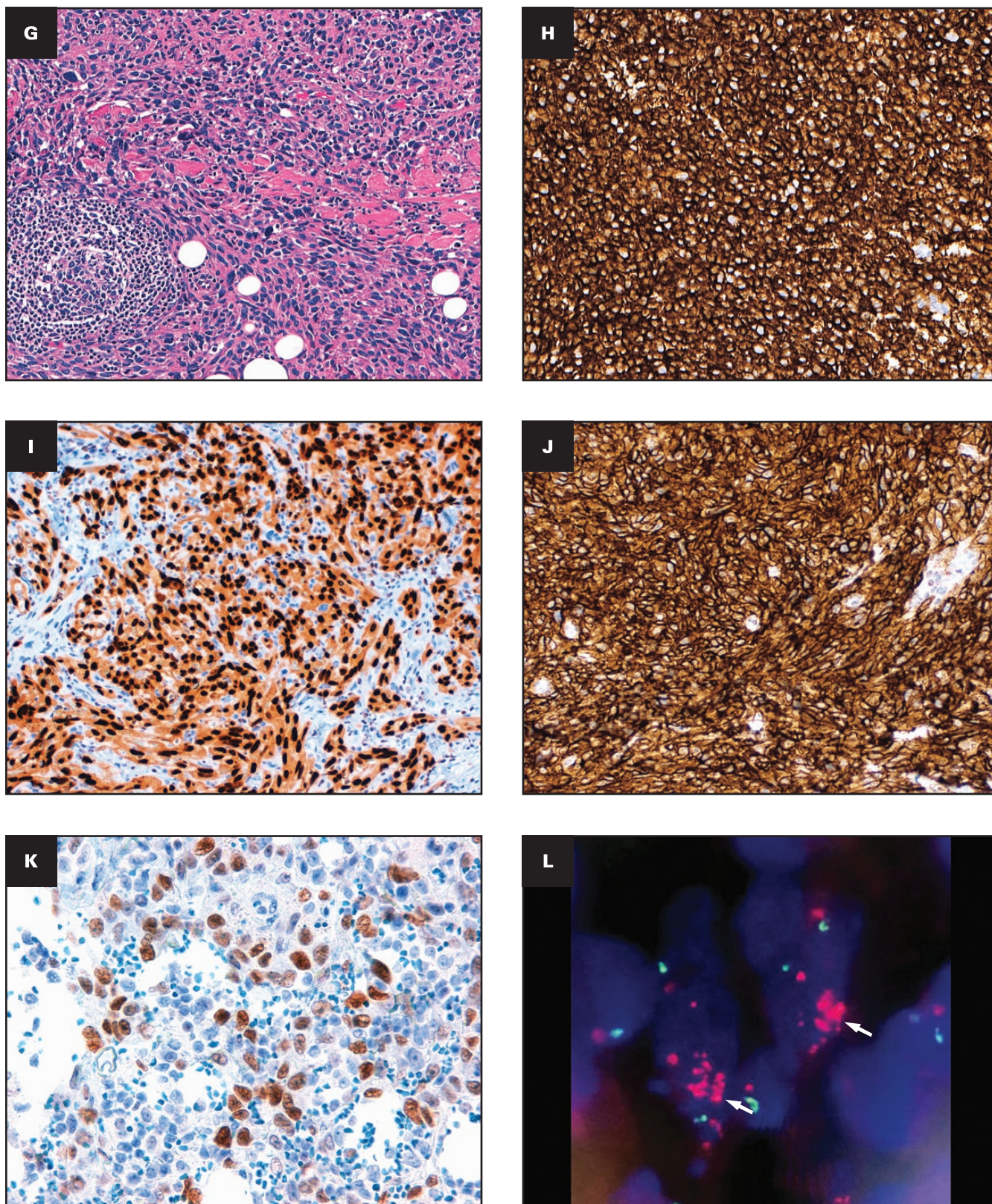


**FIGURE 1** (cont) **G**, Intratumoral lymphoid infiltrate in cutaneous angiosarcoma (H&E,  $\times 10$ ). **H**, Strong and diffuse cytoplasmic and membranous CD31 expression in angiosarcoma ( $\times 40$ ). **I**, Strong and diffuse nuclear anti-ERG immunoreactivity in angiosarcoma ( $\times 40$ ). **J**, Strong and diffuse cytoplasmic and membranous podoplanin/D2-40 expression in angiosarcoma ( $\times 40$ ). **K**, Strong and patchy nuclear MYC expression in cutaneous angiosarcoma ( $\times 40$ ). **L**, Fluorescence in situ hybridization in cutaneous postradiotherapy angiosarcoma with MYC amplification (red signals, arrows).

The HTG EdgeSeq Precision Immuno-Oncology Assay (HTG Molecular Diagnostics) characterizes the immune response in TMEs and enables the expression of hundreds of genes with minimal sample input to be measured.<sup>34-37</sup> In a recent observation from our working group, we noticed a heterogeneous lymphoid infiltration in cutaneous ASs and believed it would be interesting to explore whether the immunologic component in AS may provide additional prognostic information or be associated with an alternative therapeutic option. Immunotherapy holds substantial promise for tumors that are refractory to standard therapies and for which disease recurrence is a major clinical problem.<sup>7-34</sup> In this study, we explored features of the TME by

histology, immunohistochemistry, and HTG to define subtypes of AS that may respond to different forms of immunotherapy.

## MATERIALS AND METHODS

### Patient Selection

Formalin-fixed, paraffin-embedded (FFPE) tissue of cutaneous and noncutaneous AS (soft tissue and visceral) samples, collected from patients with AS diagnosed between 2000 and 2015, were retrieved from the Pathology Department from various hospitals in our region. The following clinical and follow-up information was obtained from medical records: patient age, sex, tumor size, clinical history, tumor location, treatment (surgery, chemotherapy, radiotherapy), type of surgery (for tumor removal), and clinical outcome (died of disease or alive). The present study was approved by the institutional review board in accordance with the ethical standards established by the investigating institution in accordance with the Declaration of Helsinki of 1975, as revised in 2008.

### Histopathology and Fluorescence In Situ Hybridization Analysis

The following histopathologic parameters (H&E) were assessed by three pathologists (I.M., F.G., and A.L.-B.) in noncutaneous and cutaneous ASs: tumor size, predominant tumor cells (epithelioid, round, spindle), necrosis, mitoses  $\times 2 \text{ mm}^2$ , and margins. Lymphoid infiltration was assessed by the same pathologists and classified as previously reported<sup>7</sup> as “immune desert” in the complete absence

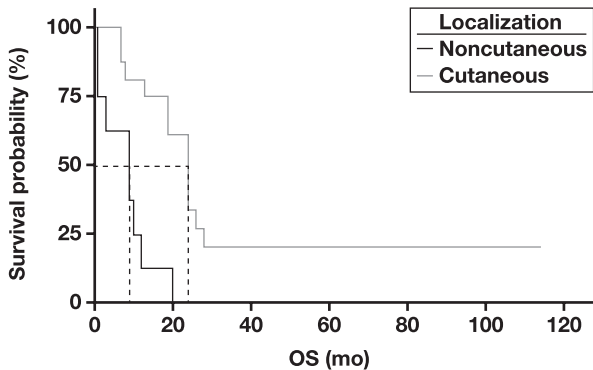


**FIGURE 2** Overall survival (OS) Kaplan-Meier curves comparing noncutaneous (n = 12) and cutaneous (n = 20) angiosarcomas. Log rank  $P = .00039$ .

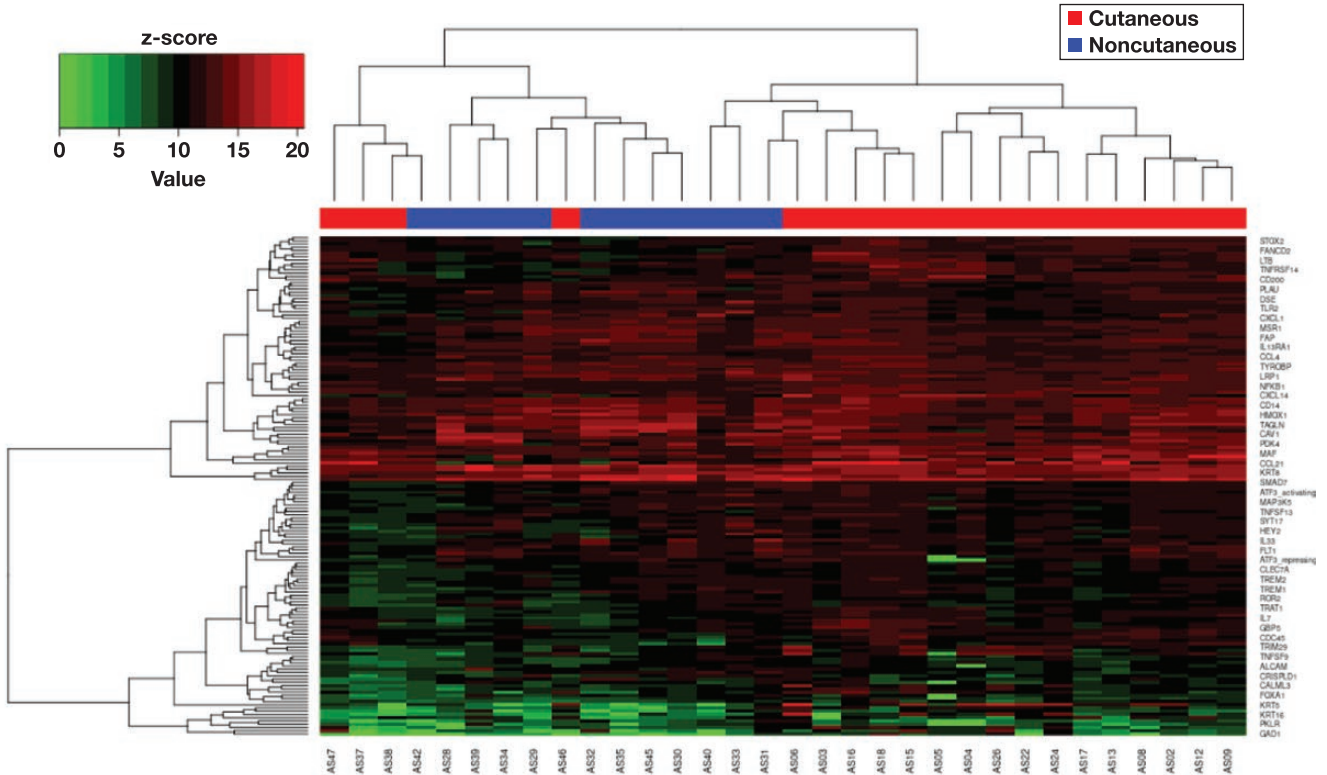


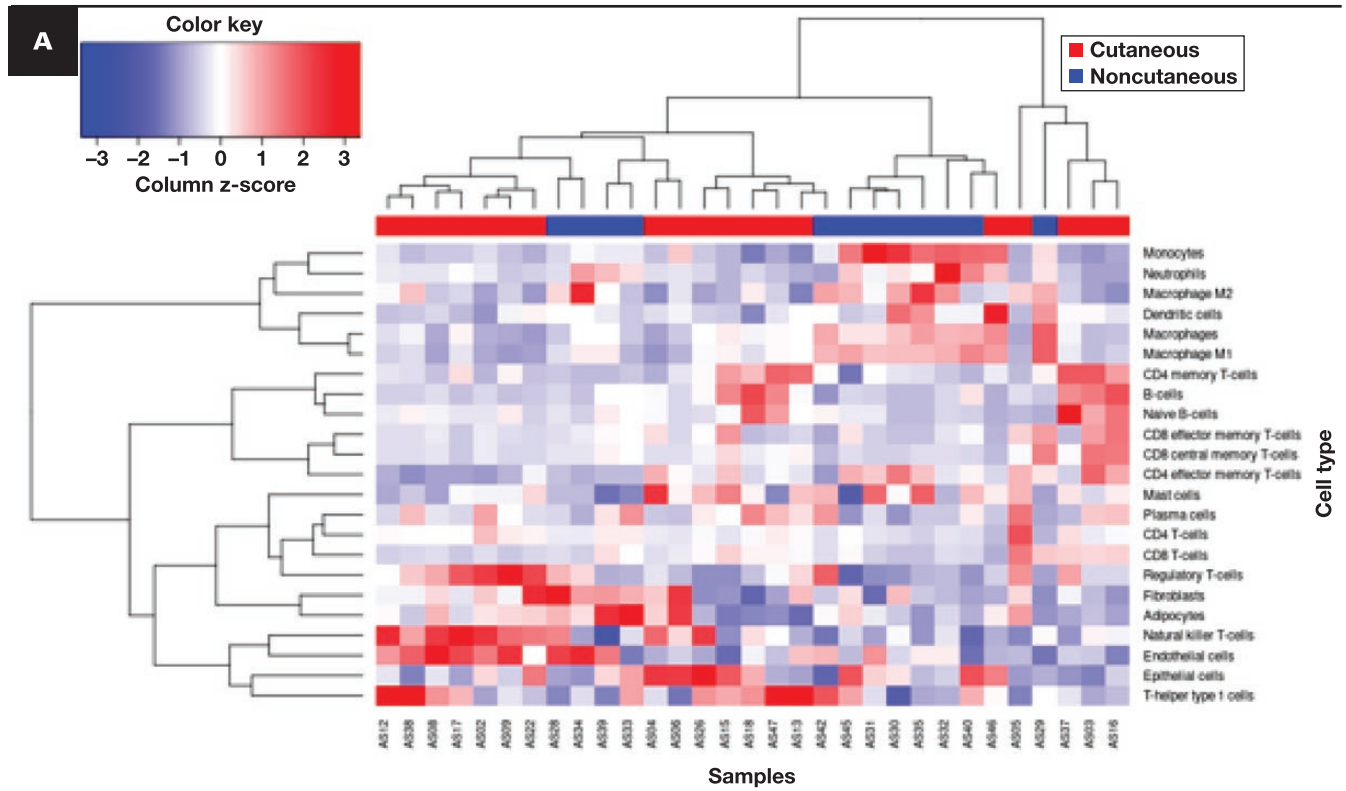
**FIGURE 3** Differential expression (DE) analysis comparing cutaneous (red; n = 20) and noncutaneous (blue; n = 12) Angiosarcomas. Unsupervised hierarchical clustering. DE genes cutaneous vs noncutaneous (155) ( $P = .1$ ).

Downloaded from https://academic.oup.com/ajcp/advance-article/doi/10.1093/ajcp/aqad003/7074437 by guest on 11 March 2023

of lymphoid infiltration, “immune excluded” if lymphoid infiltration was present exclusively at the tumor-stroma border, and “immune infiltrated” if intratumoral lymphocytes were present.

Fluorescence in situ hybridization (FISH) analysis for the quantitation of MYC was performed on FFPE tissue sections cut at 5 mm using a commercially available break-apart FISH probe set for the

MYC locus (8q24), with the 5’ probe labeled with Spectrum Red and the 3’ probe labeled with SpectrumGreen (Vysis FISH; Abbott Molecular). With this probe set, a yellow fusion signal is produced by the juxtaposition of the 5’ and the 3’ probe when the MYC locus has a normal configuration. Standard laboratory protocols and quality control measures were followed for this study. In each case, 100



**B**

| Cell type          | Noncutaneous | Cutaneous |
|--------------------|--------------|-----------|
| CD4 memory T cells |              | 0.032     |
| CD4 T cells        |              | 0.00024   |
| Macrophages M1     | 0.011        |           |
| Macrophages M2     | 0.016        |           |
| Monocytes          | 0.0099       |           |
| Naive B cells      |              | 0.033     |
| Neutrophils        | 0.0015       |           |
| NK T cells         |              | 0.025     |
| Plasma cells       |              | 0.048     |
| Regulatory T cells |              | 0.074     |

**FIGURE 4** **A**, Heatmap scores in noncutaneous (n = 12) and cutaneous (n = 20) angiosarcomas. **B**, Lymphoid and inflammatory population distribution in noncutaneous and cutaneous tumors. NK, natural killer.

interphase nuclei were analyzed in a blinded manner by two biologists (200 total nuclei). Amplification of the *MYC* locus was defined as (1) the presence of an increased number of *MYC* signals (more than 6) in tumor cells or (2) an increased number of 5' *MYC* signals (more than 4 per cell) in at least 40% in tumor cells. A clear high level of *MYC* amplification was seen in large areas, with an average of more than 20 signals per cell.

### Immuno-Oncology Panel (HTG EdgeSeq Precision Immuno-Oncology Assay)

Gene expression analysis was performed with the HTG EdgeSeq Precision Immuno-Oncology Assay (HTG Molecular Diagnostics), which characterizes the immune response in TMEs.<sup>35-38</sup> This is a novel technique consisting of a prehybridization with specific probes using a quantitative nuclease protection assay, followed by a standard RNA sequencing (RNA-seq) protocol in the Nextseq sequencer (Illumina). The main advantage of this technique is its sensitivity, since it requires very little sample input (5- $\mu$ m FFPE section). Tissue is microdissected in order to analyze only tumor tissue, and instead of analyzing the entire transcriptome, it focuses on a panel of 1,392 messenger RNAs (mRNAs) related with immune response (Precision Immuno-Oncology). The

analysis includes the main genes involved in almost all the major tumor types and implicated in the immune system.

Results are normalized to further standardize gene expression values both within and across samples. To minimize variation caused by the technology and maximize the biologic variation measured by the statistical tests, we used median normalization, as originally suggested by Anders and Huber.<sup>39</sup> Differential expression between groups in normalized data was inferred adjusting the data to a binomial negative distribution (DESeq2)<sup>8</sup> implemented in R v.4.1.2.

Baseline samples were analyzed to identify genes differentially expressed between patients in the different clinical groups. Gene set analysis was performed using the gage (Generally Applicable Gene-set/Pathway Analysis) package in R.<sup>40</sup> A visualization of the Kyoto Encyclopedia of Genes and Genomes pathways was performed with the pathview package, which maps and renders inferred data on pathway graphs.<sup>41</sup> All these analyses were performed with R v.4.1.2 and revealed differential pathway regulation between the groups.

### Immunohistochemistry Validation of Gene Expression Profile

PD-L1, PD1, CD8, and CD20 expression was examined by immunohistochemistry using the anti-PD-L1 (clone 22C3, KIT

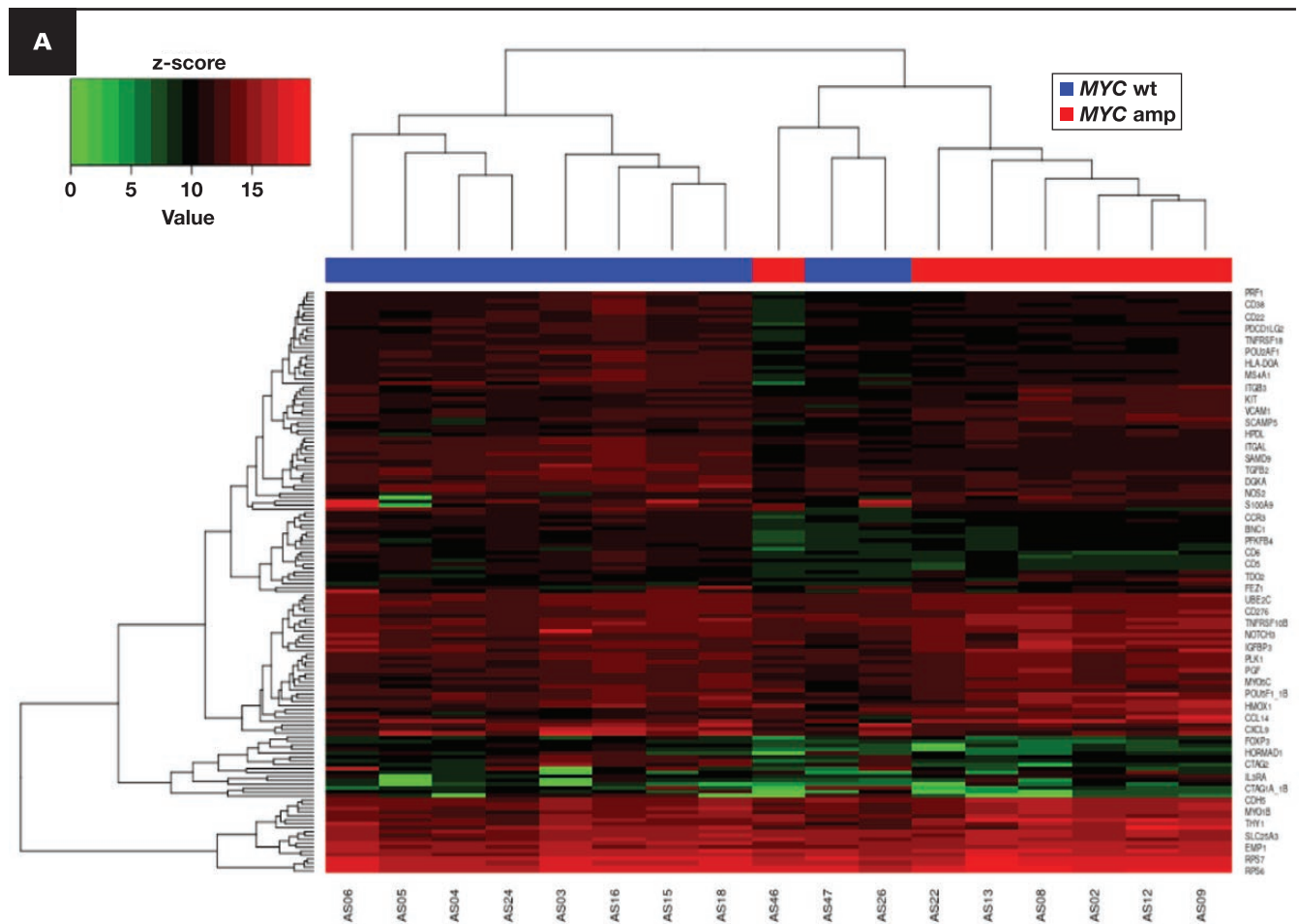


**FIGURE 5** Unsupervised hierarchical clustering comparing angiosarcomas with and without *MYC* amplification. **A**, *MYC* wt ( $n = 10$ ) vs *MYC* amp ( $n = 7$ ) (148) ( $P = .1$ ).

ready to use; Dako), PD1 (clone PA32543NAT/105, dilution 1/150; Thermo Fisher Scientific), CD8 (clone C8/144B, ready to use; Dako), and CD20 (clone L26, ready to use; Dako). Tissue samples were evaluated by two pathologists (I.M. and A.L.-B.) for expression of these four antibodies using tissue microarrays (TMAs) with three tumor cores for each tumor. The threshold for positive PD-L1 expression was greater than 1%. The tumor-infiltrating lymphocyte (TIL) score was determined by examining the immunostained TMAs. The immunohistochemistry TIL score was assigned as follows: 3 (>20 positive lymphocyte cells per high-power field), 2 (11-20 positive lymphocyte cells per high-power field), 1 (1-10 positive lymphocyte cells per high-power field), and 0 (<1 or 0 positive lymphocyte cells per high-power field). Samples with score 0 or 1 were categorized as “low immune infiltrated” and score 2 or 3 as “high immune infiltrated,” as previously described.<sup>7</sup>

### Statistical Analysis

OS curves were calculated using the log-rank test, and plots were constructed using the Kaplan-Meier method. All the statistical analyses were performed using R v.4.1.2. The OS was defined as time

from diagnosis (first biopsy) to death by any cause or until the most recent follow-up. The level of significance was defined as  $P < .05$ , and all the tests were two-tailed.

A nonparametric Mann-Whitney test was employed to compare protein expression by immunohistochemistry (PD-L1, PD1, CD8, and CD20) and gene expression by HTG.

## RESULTS

### Patient Characteristics

Thirty-two patients with AS were included. These patients were diagnosed (20 cutaneous and 12 noncutaneous) between 2000 and 2015. Patient characteristics are described in **TABLE 1**. The present study included 32 primary tumors (cutaneous and noncutaneous) as well as 8 recurrence/metastasis samples. Histological, immunohistochemical, and FISH results are summarized in **TABLE 2**. Clinical, histological, immunohistochemical, and FISH results are depicted in **FIGURE 1**.

Overall, we noted significantly better survival in patients with cutaneous ASs than noncutaneous AS,  $P = .00039$  **FIGURE 2**.

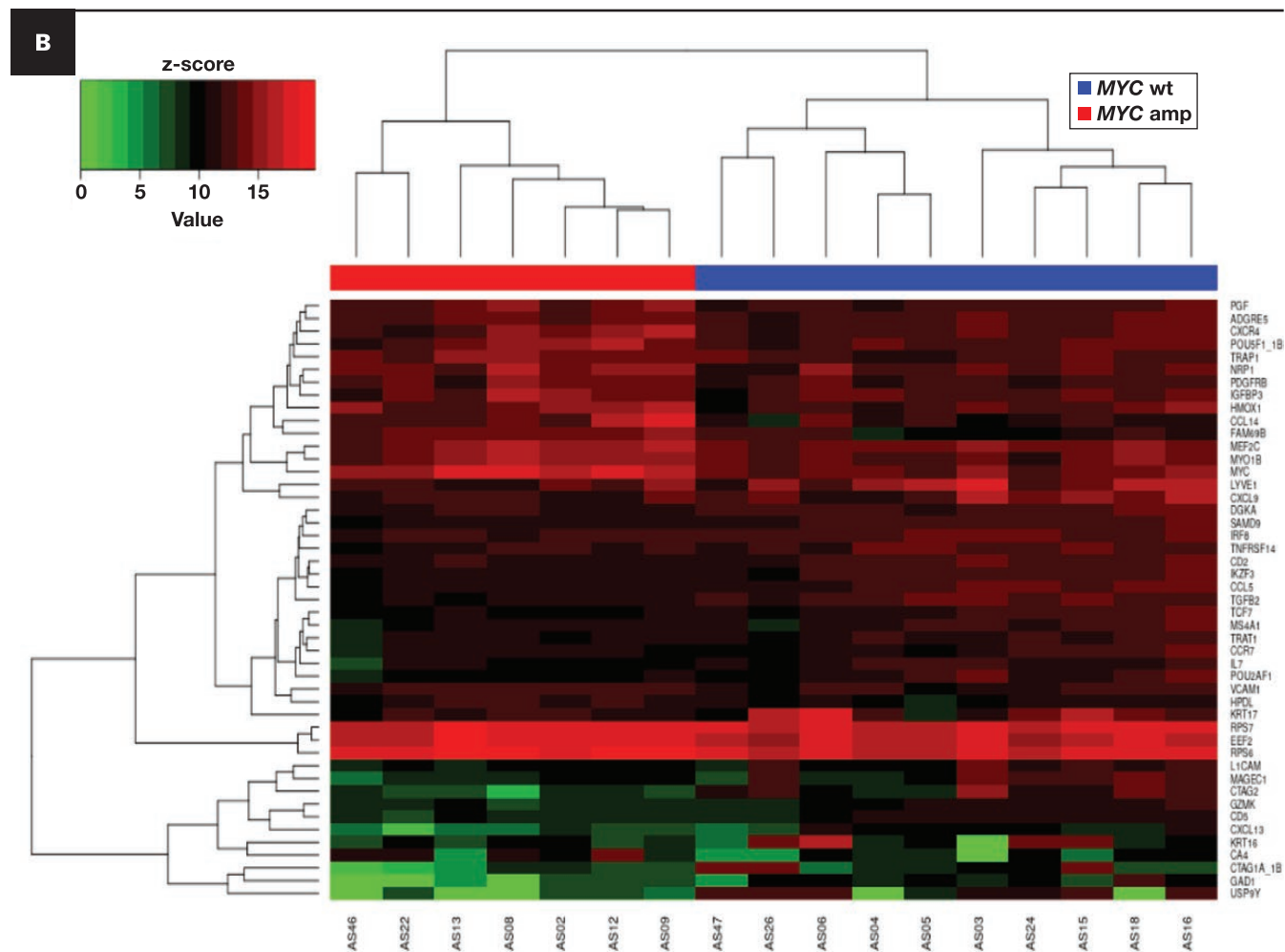


**FIGURE 5** (cont) **B**, MYC wt (n = 10) vs MYC amp (n = 7) (47) ( $P = .025$ ).

**Transcriptomic Characterization at the Immune Level**

In order to study the main clinical and biological characteristics of AS, clinical annotation was used for differential expression analysis

consisting of the following dichotomous groups: (1) cutaneous and noncutaneous ASs, (2) ASs with and without *MYC* amplification, and (3) ASs located in the head and neck area vs other anatomic sites.

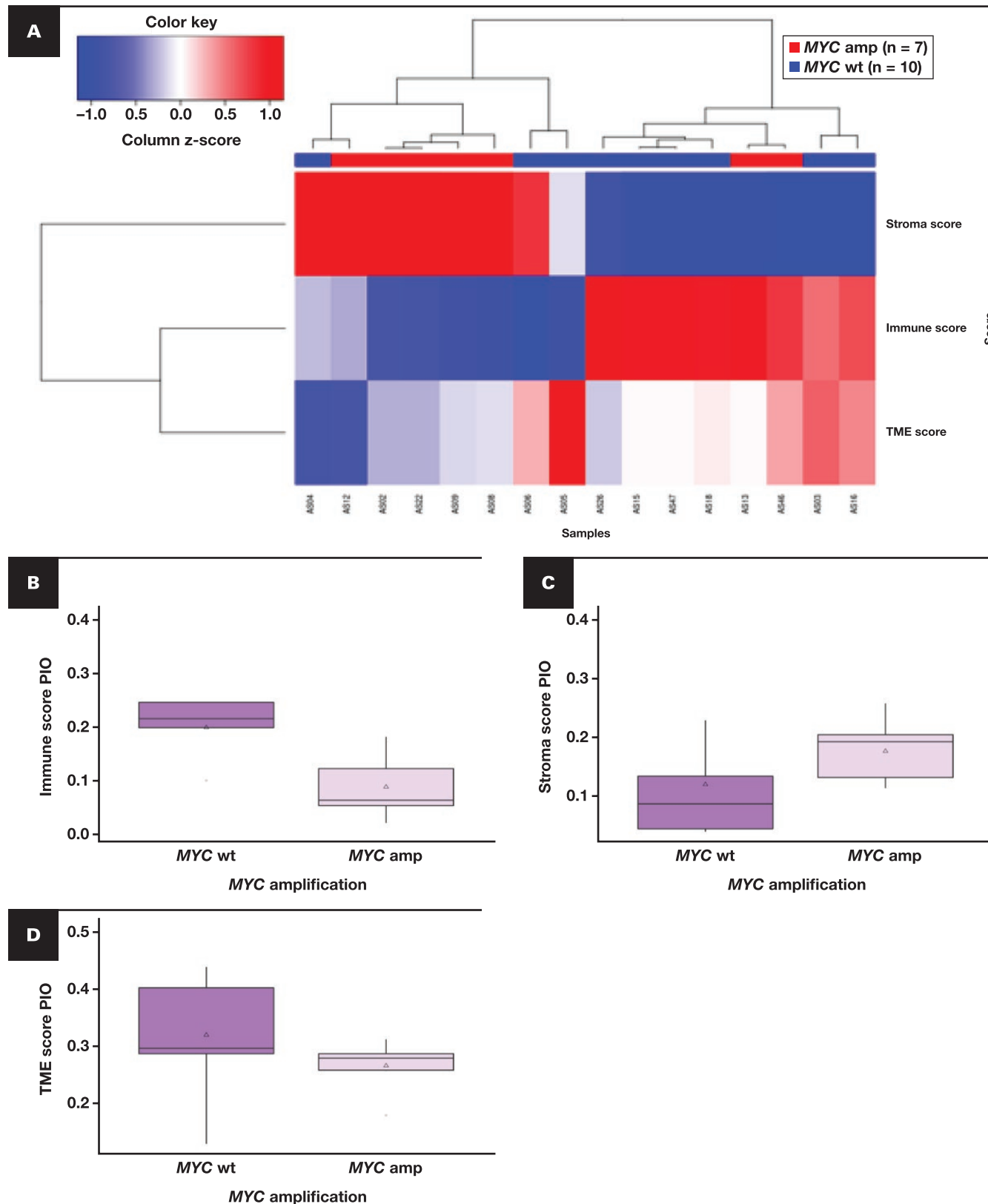


**FIGURE 6** A, Heatmap scores comparing angiosarcomas with and without *MYC* amplification. B, Immune score (*P* = .016). C, Stroma score (*P* = .14). D, Tumor microenvironment (TME) score (*P* = .17). PIO, Precision Immuno-Oncology.

### Comparison of Cutaneous (n = 20) and Noncutaneous ASs (n = 12)

Comparing cutaneous and noncutaneous ASs, the second group showed 155 deregulated genes (102 upregulated, 53 downregulated) **FIGURE 3** (Supplementary Table 1; all supplemental materials can be found at *American Journal of Clinical Pathology* online). Unsupervised hierarchical clustering distinguished two groups: the first comprised predominately cutaneous tumors, whereas the second was mainly composed of noncutaneous cases **FIGURE 3**. This genomic profile may be related to better prognosis of cutaneous subtypes likely associated with a dominant mutational signature of UV light. Gene set enrichment analysis identified phagosome, focal adhesion, extracellular matrix-receptor interaction, and complement and coagulation cascade signaling pathways as upregulated in patients with noncutaneous ASs, while the cell cycle pathway was downregulated (Supplementary Table 2).

Microenvironment cell populations were compared in the context of tumor immune and nonimmune stromal cell populations in cutaneous and noncutaneous ASs. Regarding stromal score,

immunostore, and TME score, no significant differences were found between the two groups for the three scores analyzed (Supplementary Figure 1). Nevertheless, cutaneous ASs showed a significantly higher proportion of T cells, natural killer cells, and naive B cells than noncutaneous ASs **FIGURE 4**. Furthermore, *CTLA4* was significantly more overexpressed in cutaneous ASs than in noncutaneous ASs, while PD1 and PD-L1 expression levels were similar in both cutaneous ASs and noncutaneous ASs (Supplementary Graphic 1).

### AS Without MYC Amplification (n = 10) vs AS With MYC Amplification (n = 7)

Comparing AS tumor samples with and without *MYC* amplification, 148 genes were deregulated (73 upregulated, 75 downregulated) **FIGURE 5A** (Supplementary Table 3). Unsupervised hierarchical clustering distinguished two distinct clusters, mainly with a more reduced number of genes (47 genes,  $P = .024$ ) **FIGURE 5B**. Gene set enrichment analysis identified the MAPK signaling and cell cycle pathway to be upregulated in patients with ASs with *MYC* amplification (Supplementary Table 3). Gene expression of *MYC* correlates with *MYC* genomic amplification measured by FISH (Supplementary Graphic 2).

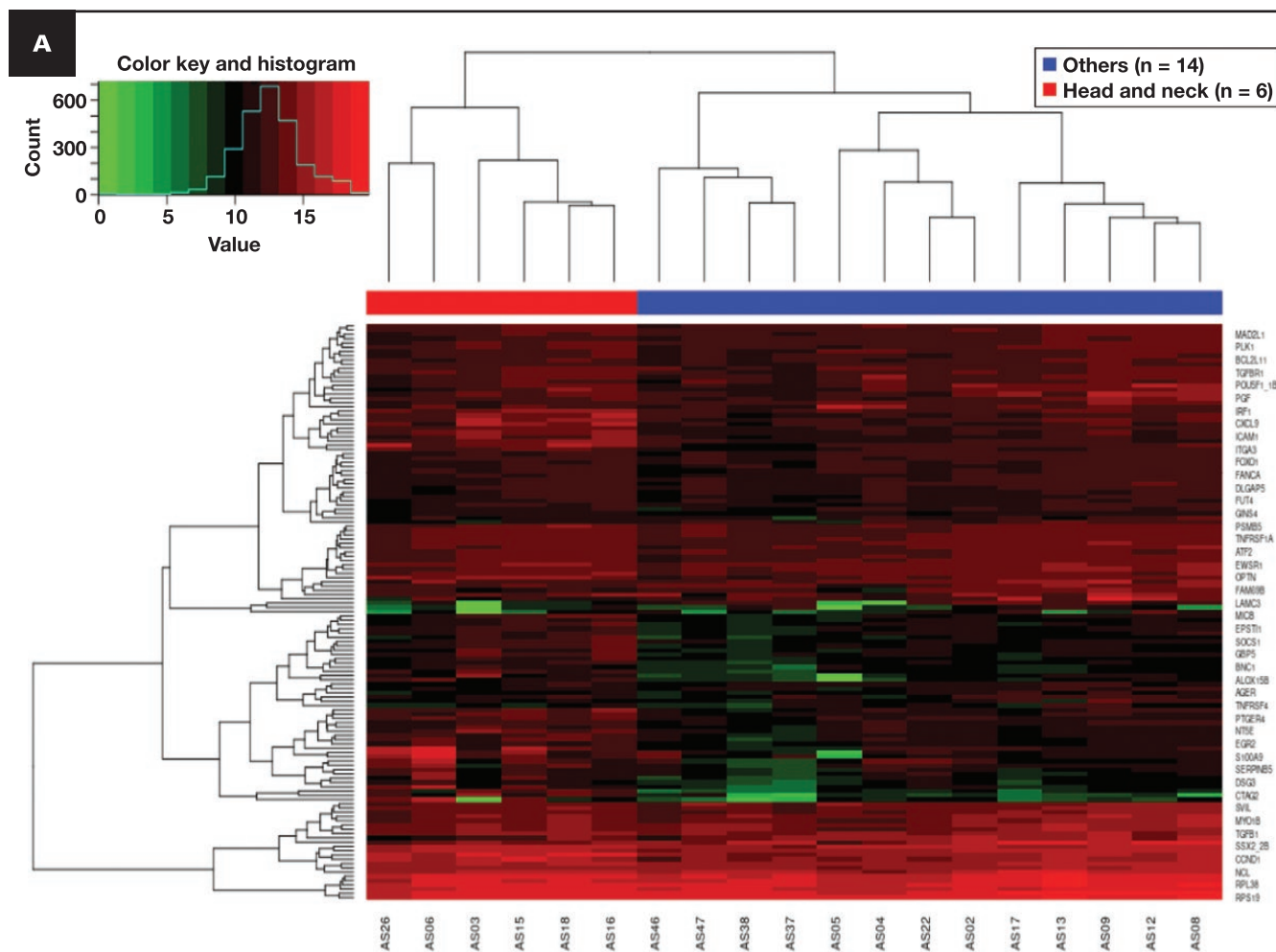


**FIGURE 7** Unsupervised hierarchical clustering comparing angiosarcomas from the head and neck area with angiosarcomas from the non-head and neck area. **A**, 135 genes ( $P = .1$ ).

Heatmaps depicting scores from both groups are summarized in **FIGURE 6**. ASs without *MYC* amplification revealed a higher immunoscore than ASs with *MYC* amplification. In addition, ASs without *MYC* amplification showed an enriched profile of CD4 and CD8 T cells as well as B cells (**Supplementary Table 4**). *PD-L1* was significantly overexpressed in ASs without *MYC* amplification, whereas *CTLA4* was significantly overexpressed in ASs with *MYC* amplification (**Supplementary Graphic 3**). Notably, all *MYC*-amplified/positive tumors were cutaneous ASs associated with previous radiotherapy in the setting of breast carcinoma.

#### Cutaneous ASs From the Head and Neck Area (n = 6) vs ASs From the Non-Head and Neck Area (n = 14)

Comparing tumor samples from the head and neck area with the non-head and neck area, 135 genes (84 upregulated, 51 downregulated) were found to be differentially expressed (**FIGURE 7** (**Supplementary Table 5**)). There were two groups in the unsupervised analysis (**FIGURE 7**). ASs from the head and neck area showed a higher immunoscore than ASs from other sites (**FIGURE 8**). In addition, ASs from the head and neck area showed a significantly higher proportion of CD8 T cells and B cells than ASs from the non-head and neck area (**Supplementary Table 6**). Furthermore, PD1 and PD-L1 content was significantly more highly expressed in ASs from the head and neck region (**Supplementary Graphic 4**).

No correlation was found between the histopathologic assessment of intratumoral lymphocytes and immunoscore, stromal score, and TME score (**Supplementary Graphic 5**).

#### Comparison Between Primary Tumors and Metastasis or Recurrence

Comparing 32 samples from primary tumors with 8 recurrence/metastasis samples, we found five differentially expressed genes (*EGRI*, *FOS*, *ID3*, *KRT5*, and *HNF1B*). There were no significant differences in scores between primary and recurrence/metastasis samples, but the last group showed an enriched profile of CD4 memory T cells, CD8 T cells, CD8 central memory T cells, macrophages, and macrophages M1.

#### Immunohistochemistry Validation of Gene Expression Profile

**FIGURE 9** and **FIGURE 10** describe protein expression in comparative groups: cutaneous vs noncutaneous AS, AS with or without *MYC* amplification, and AS from the head and neck area vs AS from the non-head and neck area. **FIGURE 11** shows a comparison between protein expression by immunohistochemistry and the corresponding gene expression profile by HTG. A significant correlation was observed with PD1, CD8, and CD20 but not with PD-L1.

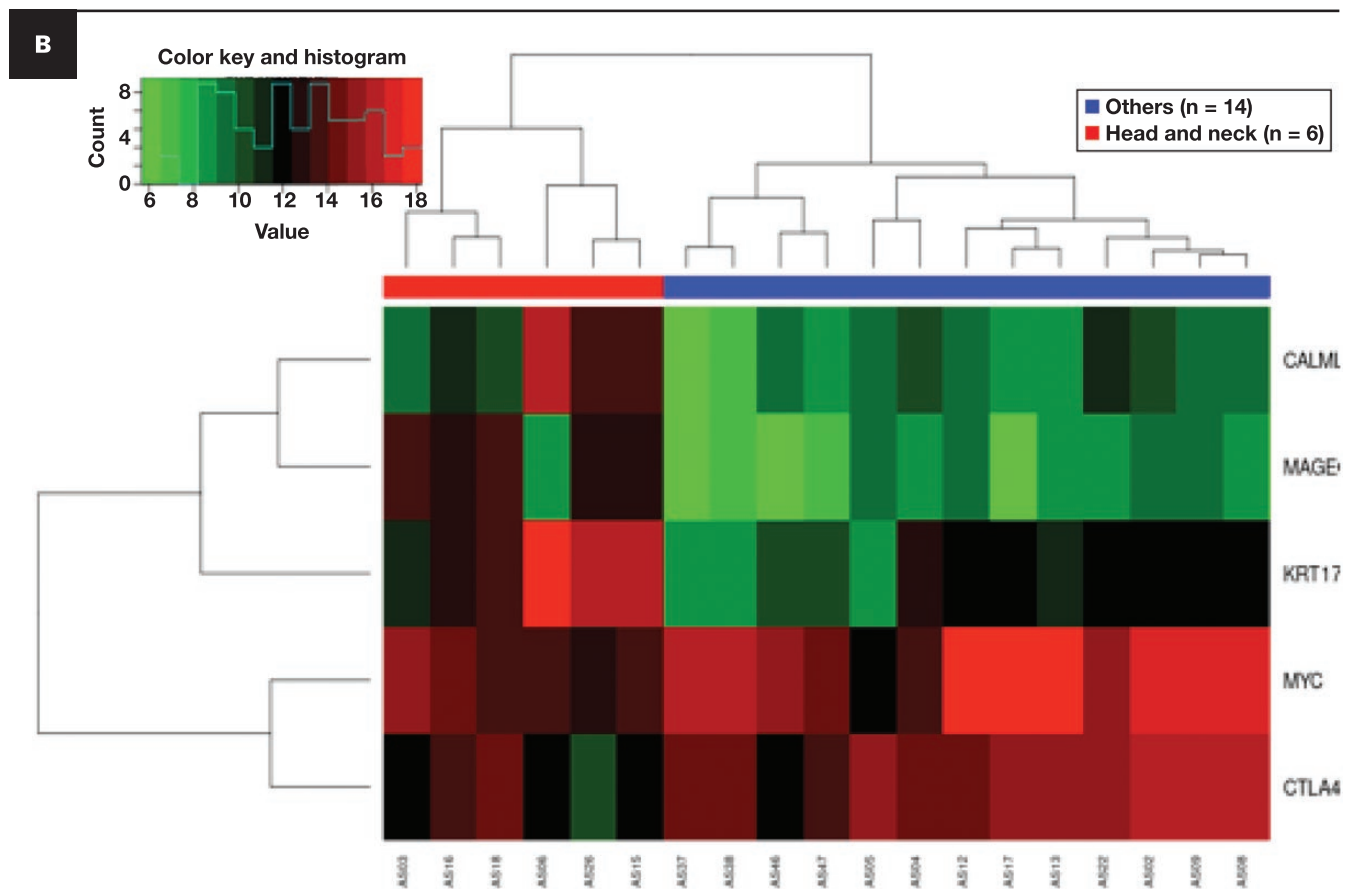


**FIGURE 7** (cont) **B**, 5 genes ( $P = .000001$ ).

**DISCUSSION**

AS is a rare histologic sarcoma subtype with significant clinical and molecular heterogeneity and poor survival.<sup>1-7</sup> Commonly, cutaneous

ASs have a different clinical course and prognosis compared with noncutaneous ASs.<sup>1-5</sup> MYC-amplified AS are mostly secondary to radiotherapy or lymphedema, and recent reports have described that

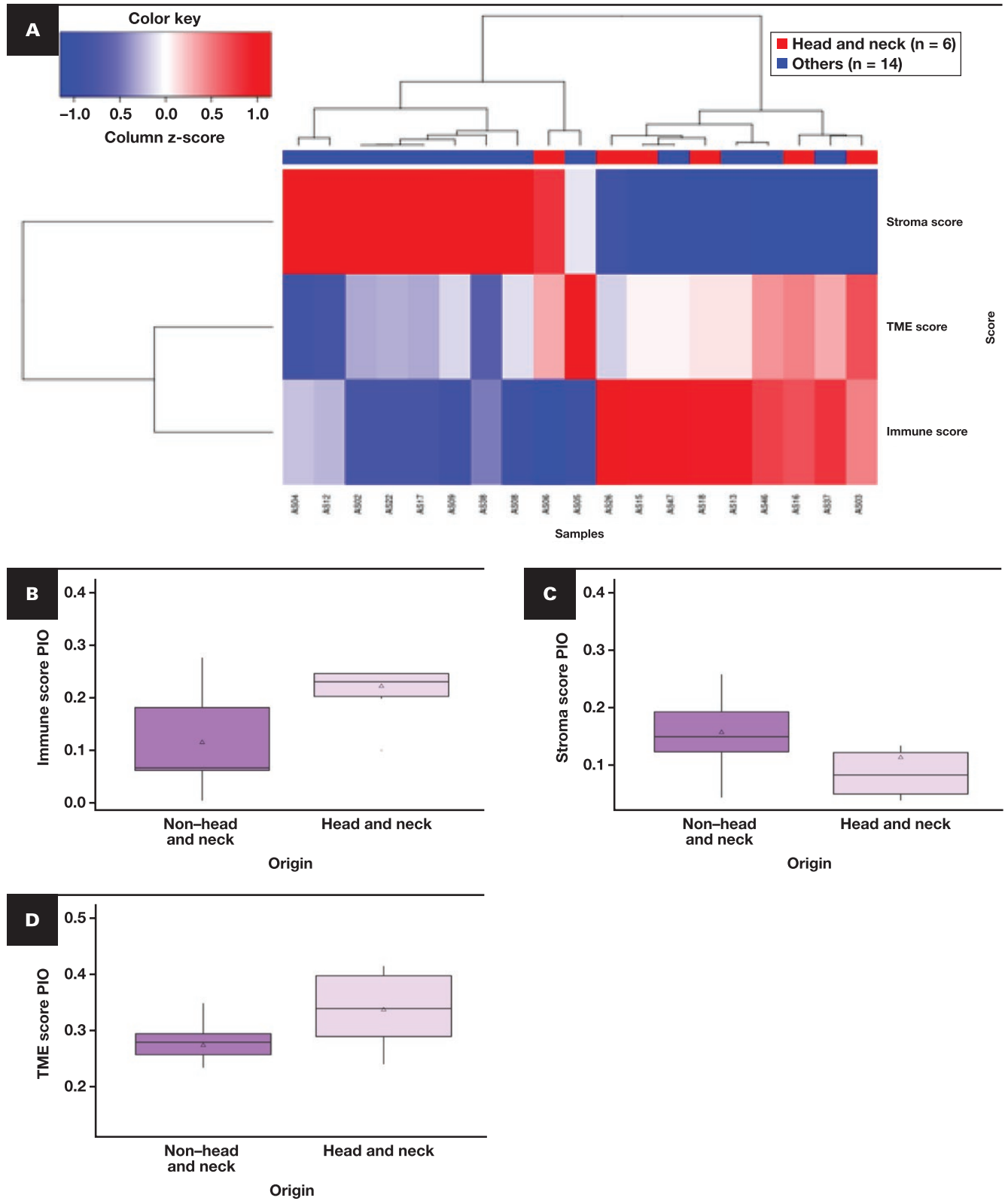


**FIGURE 8** **A**, Heatmap scores comparing from the head and neck area with angiosarcomas from the non-head and neck area. **B**, Immune score ( $P = .016$ ). **C**, Stroma score ( $P = .18$ ). **D**, Tumor microenvironment (TME) score ( $P = .13$ ). PIO, Precision Immuno-Oncology.

Downloaded from <https://academic.oup.com/ajcp/advance-article/doi/10.1093/ajcp/aqad003/7074437> by guest on 11 March 2023

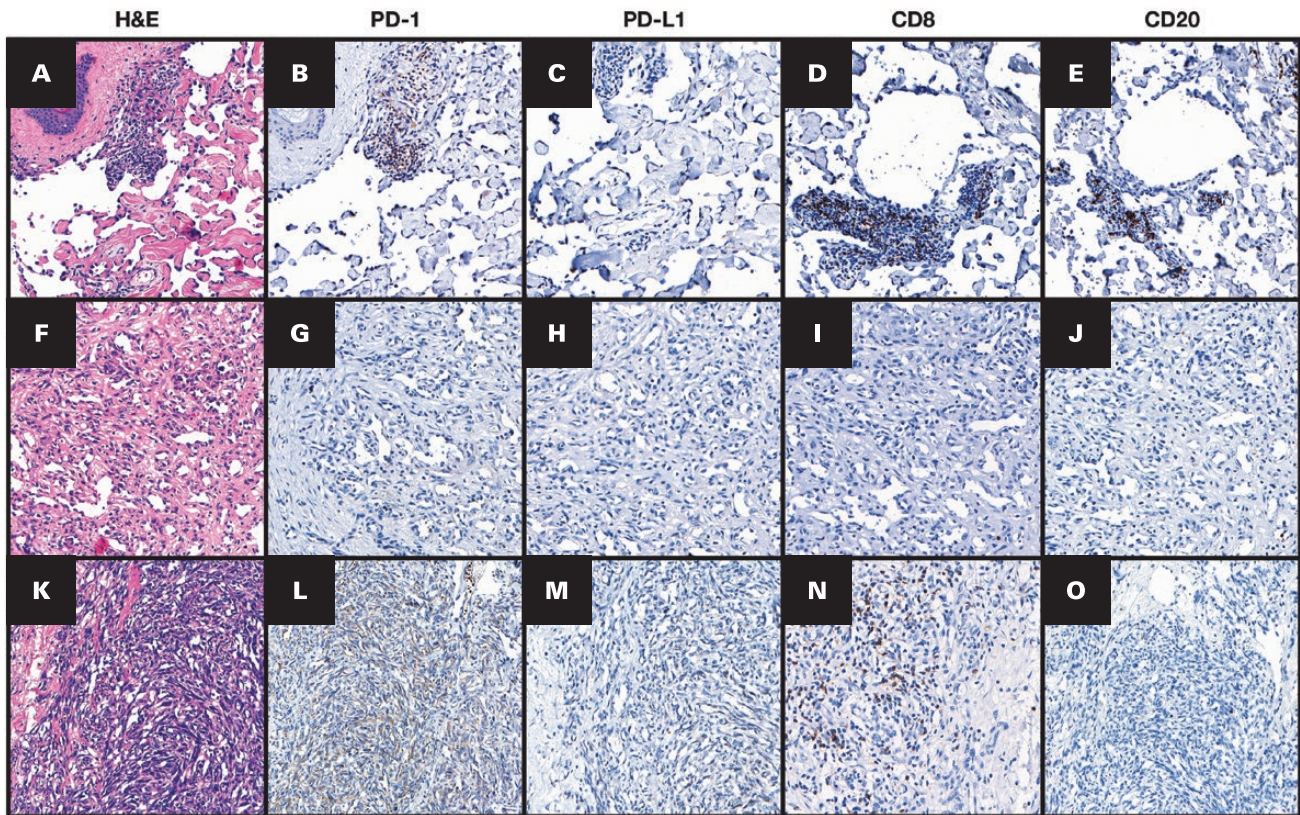


**FIGURE 9** A-E, Cutaneous angiosarcoma with high immune profile by HTG. A, H&E,  $\times 20$ . B, PD1 positive in lymphocytes,  $\times 20$ . C, PD-L1 negative,  $\times 20$ . D, CD8 positivity in tumor-infiltrating lymphocytes (TILs),  $\times 40$ . E, CD20 positive in TILs,  $\times 20$ . F-J, Noncutaneous angiosarcoma (soft tissue) with low immune profile by HTG. F, H&E,  $\times 20$ . G-J, Absent PD1, PD-L1, CD8, and CD20 expression,  $\times 40$ , respectively. K-O, Cutaneous angiosarcoma (lack of *MYC* amplification) with high immune profile by HTG. K, H&E,  $\times 40$ . L, PD1 focal expression in tumor cells,  $\times 40$ . M, PD-L1 negative,  $\times 40$ . N, CD8 immunoreactivity in TILs,  $\times 40$ . O, CD20 negative,  $\times 40$ .

AS originating in the head and neck area appears to have a better prognosis than other ASs, possibly related to the mutational profile, TMB, and the immunologic microenvironment.<sup>1-7,9-15,17-33</sup> In terms of OS, the results in the present series are fairly similar to those previously reported.<sup>1-7,9-33</sup> We have observed that cutaneous ASs had better OS than noncutaneous ASs. These findings are comparable to those found in other sarcoma series or studies, where the superficial location confers a better prognosis, probably related to the opportunity of complete resection with tumor-free margins, earlier diagnosis, less likelihood of distant dissemination, and perhaps a different immunologic microenvironment.<sup>1-7</sup>

In the present series, we profiled some of the most relevant characteristics of ASs at the immunogenomic level. To do this, we first compared the profile of differentially expressed genes in cutaneous and noncutaneous ASs, finding a signature of 155 genes. Of particular interest among these genes, *FOS* has been described as deregulated in radiation-associated AS of the breast.<sup>33</sup> Similarly, there was a profile of differentially expressed genes when comparing ASs with and without *MYC* amplification; the two groups showed evident differences, displaying a profile of 148 deregulated genes. Moreover, we also found a profile of differentially expressed genes when comparing ASs located in the head and neck area with ASs arising in other locations. The top overexpressed genes are two keratins (*KRT16* and *KRT17*) with fold changes of 44.82 and 24.35,

respectively ( $q$  value of  $1.03 \times 10^{-4}$  and  $1.23 \times 10^{-9}$ ). These last findings are in line with the results obtained in a recent study showing that ASs located in the head and neck area showed a high TMB with a different prognosis and a better response to immunotherapy,<sup>7</sup> probably related to a more immune TME.

Cutaneous ASs, ASs without *MYC* amplification, and ASs from the head and neck area showed a higher proportion of CD4 or CD8 T cells in the HTG analysis. Furthermore, ASs without *MYC* amplification and those located in the head and neck area showed a significantly higher immunoscore than ASs with *MYC* amplification and ASs arising outside the head and neck area. In addition, HTG showed significantly higher expression of *PD-L1* in ASs located in the head and neck area, as well as in ASs without *MYC* amplification. These findings are concordant with previously published results suggesting that ASs from the head and neck area appear to be more susceptible to immunotherapy, probably related to a different immunologic profile.<sup>7</sup> Moreover, larger series have reported varying levels of *PD-L1* expression, with a recent study reporting that 6 of 24 AS samples of different origins, including bone, skin, breast, soft tissue, and visceral primary tumors, had at least some membrane expression of *PD-L1*.<sup>31-33</sup> Furthermore, cutaneous ASs are known to be infiltrated with lymphocytes and to express PD1 and PD-L1. In addition, cutaneous ASs of the head and neck area may have a high TMB, likely related to a dominant mutational signature of UV



profile with the immunologic profile in AS, aiming to discover which types of AS could really benefit from immunotherapy and which would not.

The implementation of a rapid and practical immunohistochemical-based screening tool as a surrogate for gene expression profiling could be helpful to identify patients with a

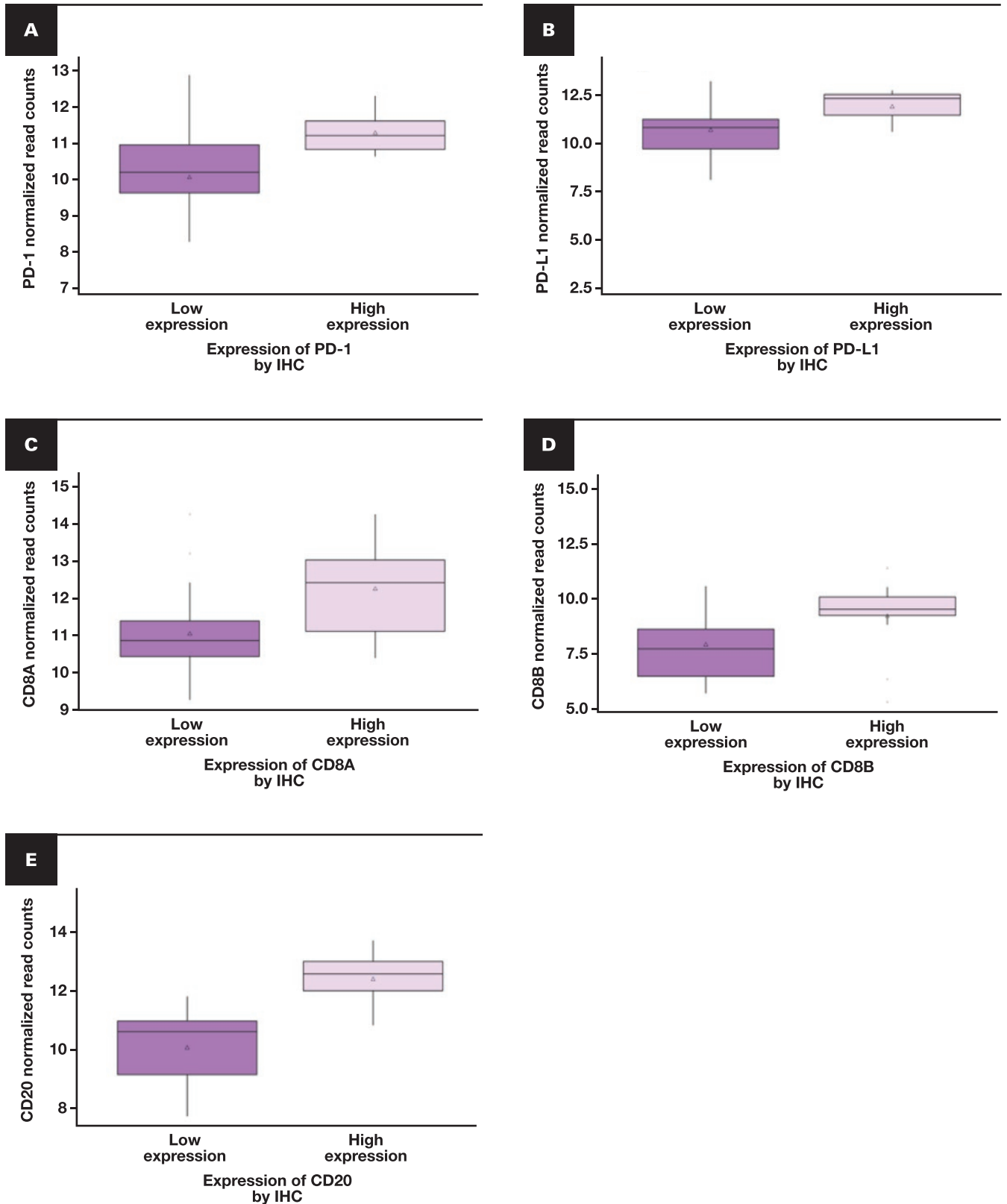


**FIGURE 11** Comparison between protein expression by immunohistochemistry (IHC) and the corresponding gene expression profile by HTG. **A**, PD-1 ( $P = .0046$ ). **B**, PD-L1 ( $P = .3$ ). **C**, CD8A ( $P = .024$ ). **D**, CD8B ( $P = .043$ ). **E**, CD20 ( $P = .00049$ ).

Downloaded from https://academic.oup.com/ajcp/advance-article/doi/10.1093/ajcp/aqad003/7074437 by guest on 11 March 2023

specific TME that may confer a more favorable response to treatment. In fact, the agreement between gene and protein expression may be influenced by several factors and includes multiple processes related to posttranscriptional regulation of gene information. The concordance in dichotomous terms for measuring the presence/absence of mRNA and protein expression ranged between 46% using microarrays and 68% using immunohistochemistry. In the present series, there was an acceptable correlation between protein expression by immunohistochemistry and gene expression in most cases, the most significant being for CD20 ( $P = .00049$ ), although it was poor for PD-L1. CD20 protein expression is easier to assess by immunohistochemistry, and PD-L1 protein expression may have been influenced by several preanalytical factors; in addition, the assessment may not be as easy as with other antibodies. A combination of an immunologic genomic profile study and immunohistochemistry assessment may provide additional information in cases of inconclusive or doubtful results.

Our HTG analyses confirmed a high degree of heterogeneity, even within the tumor immune and stromal cell compartments of this small AS series. Additional research and prospective studies with larger cohorts are needed to better understand the immune context of AS and to differentiate between the different primary sites of disease.

**Acknowledgments:** We thank Mónica Espino for valuable technical assistance with tissue microarray assembly and immunohistochemistry. This work was supported by a grant from Conselleria Sanidad, Comunidad Valenciana, 2020 (emerging groups for research). I.M. has been recognized as the first author with the award FINCIVO 2022 of the “Real Academia de Medicina de la Comunidad Valenciana (RAMCV),” Spain.

## REFERENCES

- Shustef E, Kazlouskaya V, Prieto VG, et al. Cutaneous angiosarcoma: a current update. *J Clin Pathol*. 2017;70:917-925.
- Huang SC, Zhang L, Sung YS, et al. Recurrent CIC gene abnormalities in angiosarcomas: a molecular study of 120 cases with concurrent investigation of PLAG1, KDR, MYC, and FLT4 gene alterations. *Am J Surg Pathol*. 2016;40:645-655.
- Requena C, Sendra E, Llombart B, et al. Cutaneous angiosarcoma: clinical and pathology study of 16 cases. *Actas Dermosifiliogr*. 2017;108:457-465.
- Pasquier E, André N, Street J, et al. Effective management of advanced angiosarcoma by the synergistic combination of propranolol and vinblastine-based metronomic chemotherapy: a bench to bedside study. *EBioMedicine*. 2016;6:87-95.
- Bagaria SP, Gatalica Z, Maney T, et al. Association between programmed death-ligand 1 expression and the vascular endothelial growth factor pathway in angiosarcoma. *Front Oncol*. 2018;8:71.
- Khan JA, Maki RG, Ravi V. Pathologic angiogenesis of malignant vascular sarcomas: implications for treatment. *J Clin Oncol*. 2018;36:194-201.
- Rosenbaum E, Antonescu CR, Smith S, et al. Clinical, genomic, and transcriptomic correlates of response to immune checkpoint blockade-based therapy in a cohort of patients with angiosarcoma treated at a single center. *J ImmunoTher Cancer*. 2022;10:e004149.
- Love MI, Huber W, Anders S. Moderated estimation of fold change and dispersion for RNA-seq data with DESeq2. *Genome Biol*. 2014;15:550.
- Machado I, López-Guerrero JA, Scotlandi K, et al. Immunohistochemical analysis and prognostic significance of PD-L1, PD-1, and CD8+ tumor-infiltrating lymphocytes in Ewing's sarcoma family of tumors (ESFT). *Virchows Arch*. 2018;472:815-824.
- Taube JM, Klein A, Brahmer JR, et al. Association of PD-1, PD-1 ligands, and other features of the tumor immune microenvironment with response to anti-PD-1 therapy. *Clin Cancer Res*. 2014;20:5064-5074.
- Fayette J, Martin E, Piperno-Neumann S, et al. Angiosarcomas, a heterogeneous group of sarcomas with specific behavior depending on primary site: a retrospective study of 161 cases. *Ann Oncol*. 2007;18:2030-2036.
- Fury MG, Antonescu CR, Van Zee KJ, et al. A 14-year retrospective review of angiosarcoma: clinical characteristics, prognostic factors, and treatment outcomes with surgery and chemotherapy. *Cancer J*. 2005;11:241-247.
- Antonescu CR, Yoshida A, Guo T, et al. KDR activating mutations in human angiosarcomas are sensitive to specific kinase inhibitors. *Cancer Res*. 2009;69:7175-7179.
- Behjati S, Tarpey PS, Sheldon H, et al. Recurrent PTPRB and PLAG1 mutations in angiosarcoma. *Nat Genet*. 2014;46:376-379.
- Manner J, Radlwimmer B, Hohenberger P, et al. MYC high level gene amplification is a distinctive feature of angiosarcomas after irradiation or chronic lymphedema. *Am J Pathol*. 2010;176:34-39.
- Young RJ, Natukunda A, Litière S, et al. First-line anthracycline-based chemotherapy for angiosarcoma and other soft tissue sarcoma subtypes: pooled analysis of eleven European Organisation for Research and Treatment of Cancer Soft Tissue and Bone Sarcoma Group trials. *Eur J Cancer*. 2014;50:3178-3186.
- Tawbi HA, Burgess M, Bolejack V, et al. Pembrolizumab in advanced soft-tissue sarcoma and bone sarcoma (SARC028): a multicentre, two-cohort, single-arm, open-label, phase 2 trial. *Lancet Oncol*. 2017;18:1493-1501.
- D'Angelo SP, Mahoney MR, Van Tine BA, et al. Nivolumab with or without ipilimumab treatment for metastatic sarcoma (Alliance A091401): two open-label, non-comparative, randomised, phase 2 trials. *Lancet Oncol*. 2018;19:416-426.
- Honda Y, Otsuka A, Ono S, et al. Infiltration of PD-1-positive cells in combination with tumor site PD-L1 expression is a positive prognostic factor in cutaneous angiosarcoma. *Oncoimmunology*. 2017;6:e1253657.
- Botti G, Scognamiglio G, Marra L, et al. Programmed death ligand 1 (PD-L1) expression in primary angiosarcoma. *J Cancer*. 2017;8:3166-3172.
- Wang X, Teng F, Kong L, et al. PD-L1 expression in human cancers and its association with clinical outcomes. *Onco Targets Ther*. 2016;9:5023-5039.
- Paydas S, Bagir EK, Deveci MA, et al. Clinical and prognostic significance of PD-1 and PDL1 expression in sarcomas. *Med Oncol*. 2016;33:93.
- Kim C, Kim EK, Jung H, et al. Prognostic implications of PD-L1 expression in patients with soft tissue sarcoma. *BMC Cancer*. 2016;16:434.
- Kim JR, Moon YJ, Kwon KS, et al. Tumor infiltrating PD1-positive lymphocytes and the expression of PD-L1 predict poor prognosis of soft tissue sarcomas. *PLoS One*. 2013;8:e82870.
- Raj S, Bui M, Gonzales R, et al. Impact of PDL1 expression on clinical outcomes in subtypes of sarcoma. *Ann Oncol*. 2014;25:iv498iv494-iv498iv510.
- Botti G, Scognamiglio G, Marra L, et al. Programmed death ligand 1 (PD-L1) expression in primary angiosarcoma. *J Cancer*. 2017;8:3166-3172.
- D'Angelo SP, Shoushtari AN, Agaram NP, et al. Prevalence of tumor-infiltrating lymphocytes and PD-L1 expression in the soft tissue sarcoma microenvironment. *Hum Pathol*. 2015;46:357-365.
- Shimizu A, Kaira K, Okubo Y, et al. Positive PD-L1 expression predicts worse outcome in cutaneous angiosarcoma. *J Glob Oncol*. 2016;3:360-369.
- Fujii H, Arakawa A, Utsumi D, et al. CD8+ tumor-infiltrating lymphocytes at primary sites as a possible prognostic factor of cutaneous angiosarcoma. *Int J Cancer*. 2014;134:2393-2402.

30. Sindhu S, Gimber LH, Cranmer L, et al. Angiosarcoma treated successfully with anti-PD-1 therapy a case report. *J ImmunoTher Cancer*. 2017;5:58.
31. Florou V, Rosenberg AE, Wieder E, et al. Angiosarcoma patients treated with immune checkpoint inhibitors: a case series of seven patients from a single institution. *J ImmunoTher Cancer*. 2019;7:213.
32. Painter CA, Jain E, Tomson BN, et al. The angiosarcoma project: enabling genomic and clinical discoveries in a rare cancer through patient-partnered research. *Nat Med*. 2020;26:181-187.
33. Murali R, Chandramohan R, Möller I, et al. Targeted massively parallel sequencing of angiosarcomas reveals frequent activation of the mitogen activated protein kinase pathway. *Oncotarget*. 2015;6:36041-36052.
34. Wei Y, Yang X, Gao L, et al. Differences in potential key genes and pathways between primary and radiation-associated angiosarcoma of the breast. *Transl Oncol*. 2022;19:101385.
35. Qi Z, Wang L, Desai K, et al. Reliable gene expression profiling from small and hematoxylin and eosin-stained clinical formalin-fixed, paraffin-embedded specimens using the HTG EdgeSeq platform. *J Mol Diagn*. 2019;21:796-807.
36. Zhang L, Cham J, Cooley J, et al. Cross-platform comparison of immune-related gene expression to assess intratumor immune responses following cancer immunotherapy. *J Immunol Methods*. 2021;494:113041.
37. Borchert S, Herold T, Kalbourtzis S, et al. Transcriptome-wide gene expression profiles from FFPE materials based on a nuclease protection assay reveals significantly different patterns between synovial sarcomas and morphologic mimickers. *Cancers*. 2022;14:4737.
38. Bell D, Bell A, Ferrarotto R, et al. High-grade sinonasal carcinomas and surveillance of differential expression in immune related transcriptome. *Ann Diagn Pathol*. 2020;49:151622.
39. Anders S, Huber W. Differential expression analysis for sequence count data. *Genome Biol*. 2010;11:R106.
40. Luo W, Friedman MS, Shedden K, et al. GAGE: generally applicable gene set enrichment for pathway analysis. *BMC Bioinf*. 2009;10:161.
41. Luo W, Brouwer CP. an R/Bioconductor package for pathway-based data integration and visualization. *Bioinformatics*. 2013;29:1830-1831.